



Public Health  
England



# **NHS Breast Screening Programme Equipment Report**

**Technical evaluation of IMS Giotto Class  
digital breast tomosynthesis system**

October 2018

## About Public Health England

Public Health England exists to protect and improve the nation's health and wellbeing, and reduce health inequalities. We do this through world-leading science, knowledge and intelligence, advocacy, partnerships and the delivery of specialist public health services. We are an executive agency of the Department of Health and Social Care, and a distinct delivery organisation with operational autonomy. We provide government, local government, the NHS, Parliament, industry and the public with evidence-based professional, scientific and delivery expertise and support.

Public Health England, Wellington House, 133-155 Waterloo Road, London SE1 8UG

Tel: 020 7654 8000 [www.gov.uk/phe](http://www.gov.uk/phe)

Twitter: [@PHE\\_uk](https://twitter.com/PHE_uk) Facebook: [www.facebook.com/PublicHealthEngland](https://www.facebook.com/PublicHealthEngland)

### About PHE Screening

Screening identifies apparently healthy people who may be at increased risk of a disease or condition, enabling earlier treatment or better informed decisions. National population screening programmes are implemented in the NHS on the advice of the UK National Screening Committee (UK NSC), which makes independent, evidence-based recommendations to ministers in the four UK countries. The Screening Quality Assurance Service ensures programmes are safe and effective by checking that national standards are met. PHE leads the NHS Screening Programmes and hosts the UK NSC secretariat.

[www.gov.uk/topic/population-screening-programmes](http://www.gov.uk/topic/population-screening-programmes)

Twitter: [@PHE\\_Screening](https://twitter.com/PHE_Screening) Blog: [phescreening.blog.gov.uk](http://phescreening.blog.gov.uk)

Prepared by: KC Young, JM Oduko and LM Warren

For queries relating to this document, please contact: [phe.screeninghelpdesk@nhs.net](mailto:phe.screeninghelpdesk@nhs.net)



© Crown copyright 2018

You may re-use this information (excluding logos) free of charge in any format or medium, under the terms of the Open Government Licence v3.0. To view this licence, visit [OGL](https://www.ogil.io). Where we have identified any third party copyright information you will need to obtain permission from the copyright holders concerned.

Published October 2018

PHE publications

gateway number: 2018566



PHE supports the UN

Sustainable Development Goals



# Contents

About Public Health England	2
Contents	3
Executive summary	4
1. Introduction	5
2. Methods	6
3. Results	13
4. Discussion	22
5. Conclusions	24
References	25

## Executive summary

The technical performance of the IMS Giotto Class digital breast tomosynthesis system was tested in tomosynthesis mode. The evaluation of the performance in the 2D imaging mode will be published as a separate report.

The mean glandular dose (MGD) to the standard breast in tomosynthesis mode was found to be 1.58mGy, which is below the dose limiting value of 2.5mGy in the European Reference Organisation for Quality Assured Breast Screening and Diagnostic Services (EUREF) protocol. Technical performance of this equipment was found to be satisfactory, so that the system could proceed to practical evaluation in a screening centre. This report provides baseline measurements of the equipment performance, including:

- radiation dose
- contrast detail detection
- contrast-to-noise ratio (CNR)
- reconstruction artefacts
- z-resolution
- detector response
- local dense area response

# 1. Introduction

## Testing procedures and performance standards for digital mammography

This report is one of a series<sup>1,2,3,4</sup> evaluating commercially available mammography systems on behalf of the NHS Breast Screening Programme (NHSBSP). The testing methods and standards applied are those of the relevant NHSBSP protocols, which are published as NHSBSP Equipment Reports. Report 1407<sup>5</sup> describes the testing of digital breast tomosynthesis systems.

The NHSBSP protocol is similar to the EUREF protocol,<sup>6</sup> but the latter also provides additional or more detailed tests and standards, some of which are included in this evaluation.

## Objectives

The aim of the evaluation was to measure the technical performance of the Giotto Class system in tomosynthesis mode.

## 2. Methods

### System tested

The tests were conducted at the Medical Imaging Systems (MIS) Healthcare premises in London, UK. Details of the system tested are given in **Table 1**.

**Table 1. System description**

<b>Manufacturer</b>	IMS
<b>Model</b>	Giotto Class
<b>Target material</b>	Tungsten
<b>Added filtration</b>	Silver 0.05mm
<b>Detector type</b>	Amorphous selenium
<b>Detector serial number</b>	AP01-21353
<b>Image pixel size</b>	85µm in projections 90µm for reconstructed planes
<b>Detector size</b>	240mm x 300mm
<b>Source to detector distance</b>	691mm
<b>Source to table distance</b>	672mm
<b>Automatic exposure control (AEC) modes</b>	'Dose', 'Standard', 'Contrast'
<b>Tomosynthesis projections</b>	Eleven projections without anti-scatter grid equally spaced covering range $\pm 15^\circ$
<b>Reconstructed focal planes</b>	Focal planes at 1mm intervals, number equals compressed breast thickness plus 4, using iterative reconstruction
<b>Software version</b>	Raffaello 4.4.0.0 - CANOVA 4.0.3.2 - IMSTomoProc 4.3.2 (WL) - IMSProc 4.3.0.0)

Images were available in standard Breast Tomosynthesis digital imaging and communications in medicine (DICOM) format, but CT format can also be configured on the system.

The system was tested in 'Standard' AEC configuration. However, 'Dose' and 'Contrast' AEC configurations can also be set. The other dose levels are a fixed ratio compared to that computed for the standard AEC mode - "Dose" =  $0.85 \times \text{Standard}$ , "Contrast" =  $1.30 \times \text{Standard}$  (this information was provided by the manufacturer after testing).

Images can be acquired in 'QC mode' or 'clinical mode'. The standard reconstruction is at 1mm intervals. For this evaluation, reconstructions at an interval of 0.5mm and slabs of 10mm were provided. The default for reconstructions for tomosynthesis-guided biopsy is an interval of 0.5mm and this option is only available on biopsy-enabled systems. Slab reconstruction will be

available on clinical units, and the slab thickness can be customised between 2mm and 10mm according to customer needs.

There is a facility available to carry out a combination exposure, in which 2D and tomosynthesis exposures are performed within a single compression.

Approximate files sizes given in Table 2 were taken from the CDMAM images in QC mode, with a compressed breast thickness of 46mm. Note that the file size will vary depending on breast thickness and field size.

**Table 2. Image file sizes for 46mm compressed breast thickness**

<b>Image Type</b>	<b>Plane interval</b>	<b>Approximate file size</b>
Projections	N/A	216MB (total for 11 projections)
Reconstructed planes	1mm spacing	638MB
Reconstructed planes	0.5mm spacing	1300MB
Reconstructed planes	10mm spacing	129MB

An image of the Giotto Class is shown in **Figure 1**.



**Figure 1. The Giotto Class digital breast tomosynthesis system**

## Dose and contrast-to-noise ratio under AEC

### Dose measurement

To calculate the MGD to the standard breast, measurements were made of half-value layer (HVL) and tube output, across the clinically relevant range of kV and filter combinations. The output measurements were made on the midline at the standard position of 40mm from the chest wall edge (CWE) of the breast support platform. The stationary exposure option was selected for these measurements.

In tomosynthesis mode, exposures of a range of thicknesses of polymethyl methacrylate (PMMA) were made using AEC. For each measurement the height of the paddle was set to match the indicated thickness to the equivalent breast thickness for that thickness of PMMA. The method described in the UK protocols<sup>5</sup> for measuring MGD requires the incident air kerma to be measured with the compression paddle well above the ion chamber. Here the method described by Dance et al<sup>7</sup> was used, in which the incident air kerma is measured with the compression paddle in contact with the ion chamber. Measurements on other systems 1, 2 show that this variation increases the air kerma measurement by 3% to 5%.

The equation used to calculate tomosynthesis MGD is shown in Equation 1

$$D=KgcsT \quad (1)$$

Where  $D$  is the MGD,  $K$  is the air kerma measured at the entrance surface of the breast,  $g$ ,  $c$  and  $s$  are dose correction factors for 2D mammography and  $T$  is a correction factor for tomosynthesis.

### Contrast-to-noise ratio

For contrast-to-noise ratio (CNR) measurements a 10mm x 10mm square of 0.2mm thick aluminium foil was included in the PMMA phantom, positioned 10mm above the table on the midline, 60mm from the CWE.

CNR was assessed using 5mm x 5mm return on investments (ROIs) positioned in the centre of the aluminium square and two background positions, to the chest wall and nipple sides of the square, as shown in Figure 2. The CNR was measured in the focal plane in which the aluminium square was brought into focus. CNR was also assessed in the unprocessed tomosynthesis projections acquired for the above images, using a 5mm x 5mm ROI.

Variation of CNR with dose was assessed in the reconstructed focal planes for a simulated standard breast thickness of 53mm (45mm PMMA). The variation in central projection CNR with breast thickness and the variation in projection CNR with projection angle for a 53mm breast were also assessed.



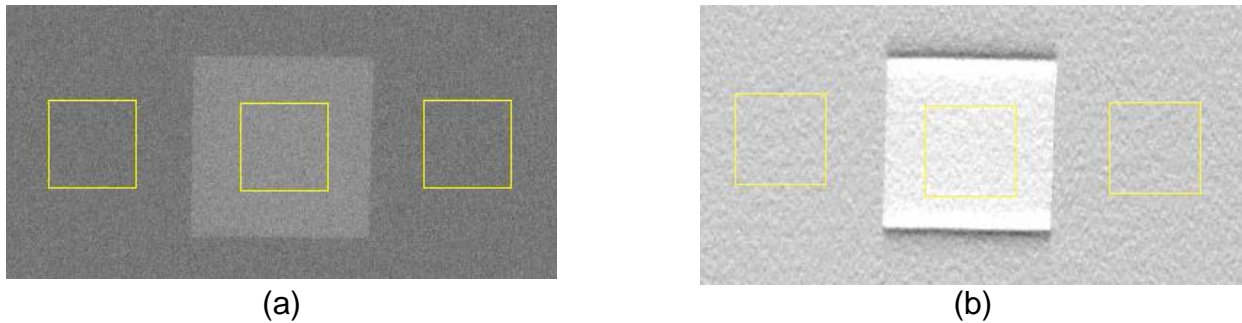


**Figure 2. Location of 5mm x 5mm ROIs for assessment of CNR. The chest wall edge is to the right of each image (a) Central projection (b) Reconstructed plane**

### Image quality measurements

In the absence of a more suitable test object for assessing tomosynthesis imaging performance, images of the CDMAM phantom were acquired in tomosynthesis mode. The CDMAM phantom (version 3.4, serial number 1022) was sandwiched between 2 blocks of PMMA, each of which was 20 mm thick. The exposure factors used were the same as would be selected by the AEC for an equivalent breast thickness of 60mm. A set of 16 images was acquired at the AEC selected dose level, in QC mode. Two further sets of 8 images at double and half the AEC selected dose level were acquired in QC mode. A further set of 8 images were acquired at the AEC selected dose level, in clinical mode.

For the AEC selected dose level, in addition to the typical 1mm spacing, reconstructed images were provided after testing at a spacing of 0.5mm and slabs of thickness 10mm.

The focal plane corresponding to the vertical position of the CDMAM phantom within the image was extracted from each reconstructed stack of images. The sets of CDMAM images were read and analysed using 2 software tools: CDCOM version 1.6 ([www.euref.org/downloads](http://www.euref.org/downloads)) and CDMAM Analysis version 2.1 from the National Coordinating Centre for the Physics of Mammography (NCCPM), Guildford (<https://medphys.royalsurrey.nhs.uk/nccpm/?s=cdmam-analysis>). This was repeated for 2 focal planes immediately above and below the expected plane of best focus to ensure that the threshold gold thickness quoted corresponded to the best image quality obtained (in plane in best focus).

### 2.4 Geometric distortion and reconstruction artefacts

The relationship between reconstructed tomosynthesis focal planes and the physical geometry of the volume that they represent was assessed. This was done by imaging a geometric test phantom consisting of a rectangular array of 1mm diameter aluminium balls at 50mm intervals in the middle of a 5mm thick sheet of PMMA. The phantom was placed with the balls at various heights (7.5mm, 27.5mm, and 52.5mm) above the breast support table within a 60mm stack of plain sheets of PMMA. Reconstructed tomosynthesis planes were analysed to find the height of the focal plane in which each ball was best in focus, the position of the centre of the ball within

that plane, and the number of adjacent planes in which the ball was also seen. The variation in appearance of the ball between focal planes was quantified.

This analysis was automated using a software tool developed at NCCPM for this purpose. (<https://medphys.royalsurrey.nhs.uk/nccpm/?s=tomosynthesisqctools>). This software is in the form of a plug-in for use in conjunction with ImageJ (<http://rsb.info.nih.gov/ij/>).

#### 2.4.1 Height of best focus

For each ball, the height of the focal plane in which it was best in focus was identified. Results were compared for all balls within each image to judge whether there was any variation, indicating possible tilt of the test phantom relative to the reconstructed planes or any vertical distortion of the focal planes within the image.

#### 2.4.2 Positional accuracy within focal plane

The x and y co-ordinates within the image were found for each ball (x and y are perpendicular and parallel to the CWE, respectively). The mean distances between adjacent balls were calculated, using the pixel spacing quoted in the DICOM image header. This was compared to the physical separation of balls within the phantom, to assess the scaling accuracy in the x and y directions. The maximum deviations from the mean x and y separations were calculated, to indicate whether there was any discernible distortion of the image within the focal plane.

#### 2.4.3 Appearance of the ball in adjacent focal planes

Changes to the appearance of balls between focal planes were assessed visually and are described in the results section of this report.

To quantify the extent of reconstruction artefacts in focal planes adjacent to those containing the image of the balls, the reconstructed image was treated as though it were a true 3-dimensional volume. The software tool was used to find the z-dimension of a cuboid around each ball which would enclose all pixels with values exceeding 50% of the maximum pixel value. The method used was to re-slice the image vertically and create a composite x-z image using the maximum pixel values from all re-sliced x-z focal planes. A composite z line was then created using the maximum pixel from each column of the x-z composite plane, and a full width at half maximum (FWHM) measurement in the z-direction was made by fitting a polynomial spline. All pixel values were background subtracted using the mean pixel value from around the ball in the plane of best focus. The composite z-FWHM thus calculated (which depends on the size of the imaged ball) was used as a measure of the inter-plane resolution, or z-resolution.

## 2.5 Alignment

Alignment measurements were carried out for reconstructed tomosynthesis images.

The alignment of the X-ray beam to the focal plane at the surface of the breast support table was assessed. Self-developing film and graduated markers were positioned at the edges of the X-ray beam. Because the light beam indicated a large penumbra, the front collimator position was adjusted several times in an attempt to avoid both overshoot of the X-ray beam, and under-coverage of the detector. Measurement at the front edge was later repeated after a modification of the collimator position in the tube head.

The alignment of the imaged volume to the compressed volume was also assessed. Small high-contrast markers were placed on the breast support table and on the underside of the compression paddle to assess vertical alignment. The image planes were then inspected to check whether all markers were brought into focus within the reconstructed tomosynthesis volume. This was performed with a flat paddle and also with a 2mm spacer at the chest wall edge to give some tilt.

## 2.6 Repeatability and image uniformity

The repeatability of the tomosynthesis exposures was tested by acquiring a series of 5 images of a 45mm thick block of PMMA under AEC. The exposure factors selected by the AEC for each image were obtained from the DICOM header for each image.

The set of 16 tomosynthesis CDMAM images was used to test the repeatability of the reconstructed tomosynthesis images. The signal-to-noise ratio (SNR) was calculated just outside the CDMAM grid, in the same position in the in-focus plane, from each reconstructed image.

A combination exposure was carried out to test whether the exposure factors matched those for separate 2D and tomosynthesis exposures.

Tomosynthesis images of 45mm PMMA were assessed for uniformity.

## 2.7 Detector response

The detector response was measured as described in the NHSBSP protocol, but with a 2mm thick aluminium filter at the tube head, and beam quality as for a 90mm thick compressed breast. Images were acquired with zero degrees tomosynthesis acquisition.

Using a 10mm x 10mm ROI positioned on the midline 60mm from the chest wall edge of the central projection image, measurements were made of the mean pixel value, which was plotted against air kerma incident at the detector.

## 2.8 Timings

Using a stopwatch image timings were measured whilst imaging a 53mm equivalent breast, simulated using 45mm PMMA, under AEC. Scan times were measured, from when the exposure button was pressed until the compression paddle was released. Also measured was the time from decompression until the reconstructed tomosynthesis view was displayed on the acquisition workstation.

## 2.9 Local dense area

The local dense area test was carried out as described in the EUREF protocol. 6 A 40mm thickness of PMMA was placed on the breast support table and the compression paddle was positioned at a height of 40mm. Additional small pieces of PMMA (20mm x 40mm) were placed on top of the paddle, on the midline at 50mm from the chest wall edge, to create an additional thickness of up to 14mm. For each thickness exposure factors were recorded under AEC control.

In the simulated local dense area, the mean pixel value and standard deviation for a 10mm x 10mm ROI were measured and the signal-to-noise ratios (SNRs) were calculated for the projection images.

## 2.10 Test for radiation safety

The AEC back-up timer was tested.

### 3. Results

#### 3.1 Dose and contrast to noise ratio using AEC

The measurements of HVL and tube output are summarised in Table 3.

**Table 3. HVL and tube output measurement in tomosynthesis mode**

kV	Anode / Filter	HVL (mm Al)	Output ( $\mu\text{Gy/mAs}$ at 1m)
25	W/Ag	0.49	14.31
28	W/Ag	0.57	21.56
31	W/Ag	0.62	28.53
34	W/Ag	0.65	35.70

Calculated MGD to the standard breast model for AEC exposures in tomosynthesis mode are shown in Figure 3 and Table 4.

In the combination exposure mode, for the 2D component, with 45mm PMMA and a CBT of 53mm, the AEC selected 29kV and 57mAs, corresponding to a MGD of 1.01mGy. For 2D mode, the AEC selected 30kV and 55mAs corresponding to a MGD of 1.10mGy.

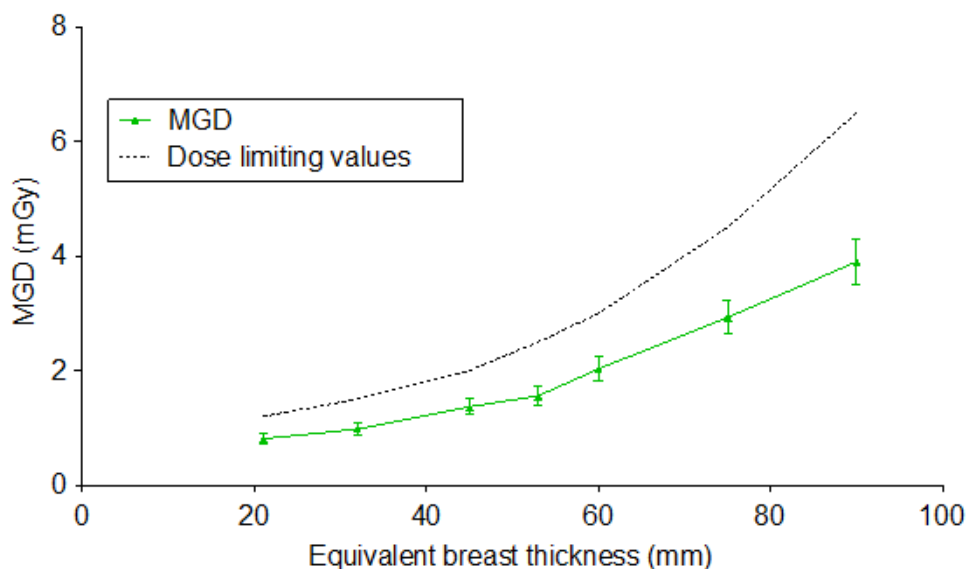


**Figure 3. Mean glandular doses (including pre-pulse) to the standard breast model. Error bars indicate 95% confidence limits**

The CNR measured in focal planes for different thicknesses of PMMA are shown in Figure 4. Figure 5 shows the CNR of the central projection image, for different thicknesses of PMMA. Figure 6 shows the CNR in the projection images at different projection angles for a 45mm thickness of PMMA.

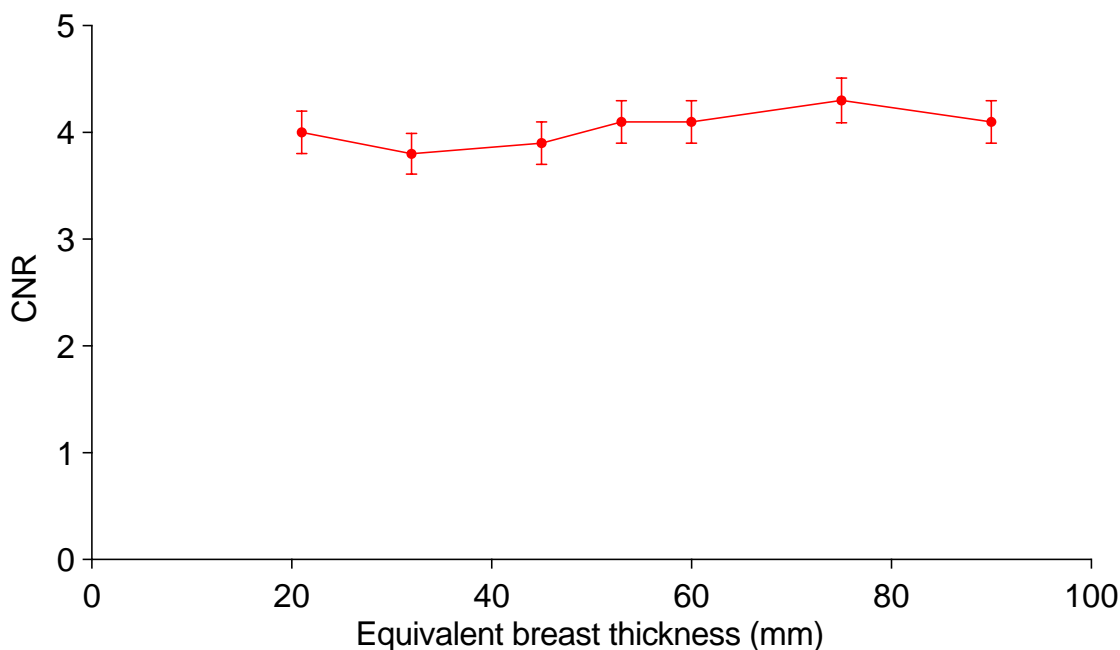


**Figure 4. CNR for tomosynthesis planes obtained under AEC. Error bars indicate 95% confidence limits**

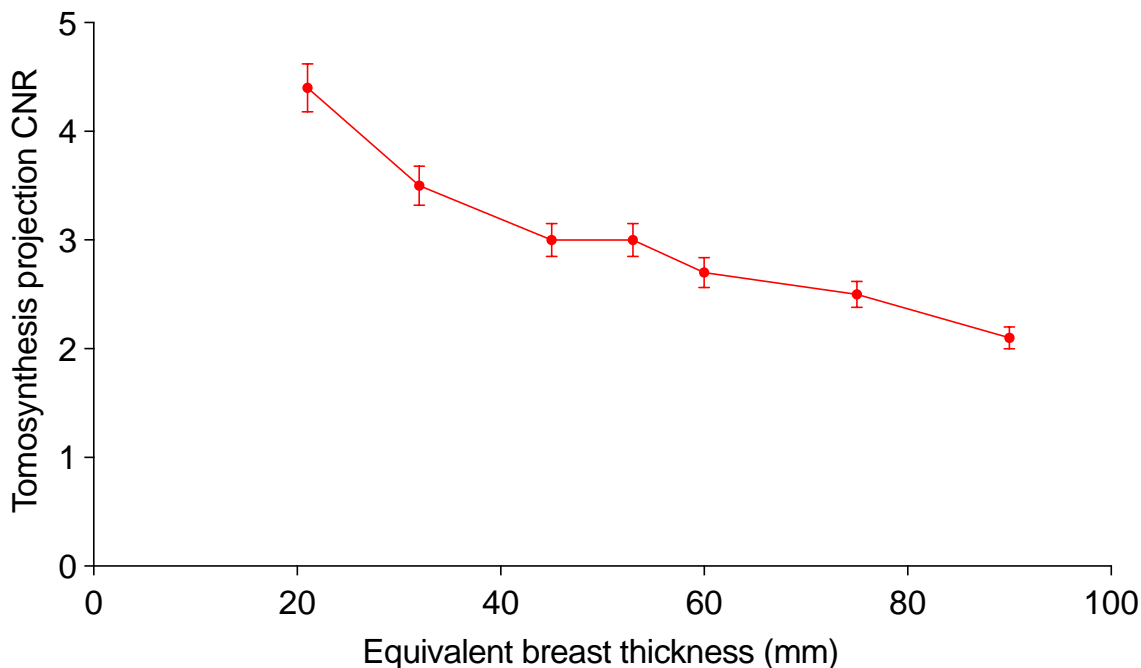


**Figure 5. CNR for tomosynthesis central projection images obtained under AEC. Error bars indicate 95% confidence limits**

The MGD and CNR results shown in Figures 3, 4 and 5 are listed in Table 4. All MGD values quoted include the preliminary exposure, which is included in the image. The radiographic factors selected for the pre-pulse are shown in Table A.1 in the Appendix.

**Table 4. Dose and CNR for tomosynthesis images under AEC**

PMMA thickness (mm)	Equivalent breast thickness (mm)	kV	Target/filter	mAs	MGD (mGy)	CNR projections	CNR planes
20	21	25	W/Ag	49.4	0.82	4.4	4.0
30	32	26	W/Ag	62.1	1.00	3.5	3.8
40	45	28	W/Ag	74.3	1.39	3.0	3.9
45	53	29	W/Ag	80.3	1.58	3.0	4.1
50	60	31	W/Ag	88.3	2.07	2.7	4.1
60	75	32	W/Ag	129.9	2.98	2.5	4.3
70	90	34	W/Ag	167.8	3.98	2.1	4.1

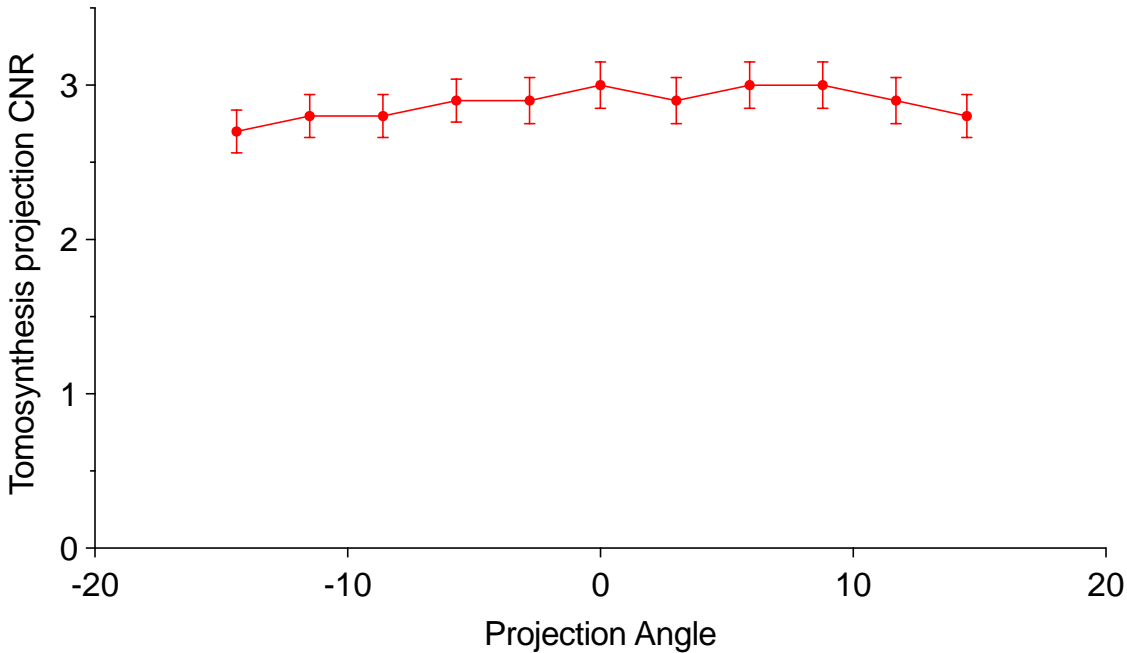


**Figure 6. Variation of projection CNR with angle for images of 45mm PMMA. Error bars are 5% of the mean value**

### 3.2 Image quality measurements

The lowest threshold gold thicknesses were obtained for focal plane 23. Figure 7 shows the threshold gold thickness detail detection curves for focal plane 23 at the AEC dose level, and half and double the AEC level, all in QC mode. The curve at the AEC dose level is also shown for the ‘clinical’ mode. The CDMAM results shown in Figure 7 are summarised in Table 5.

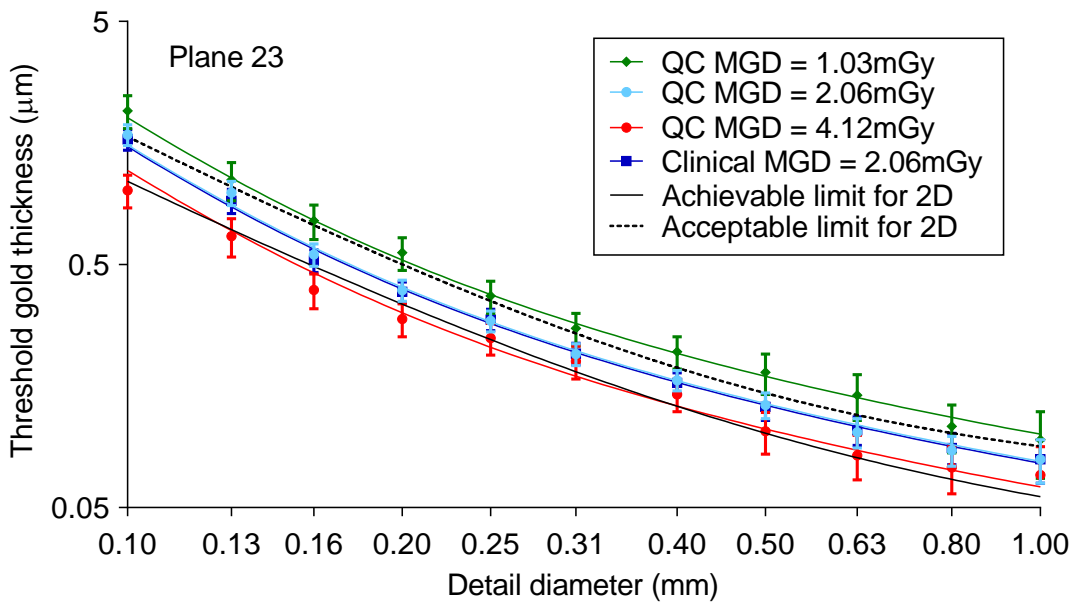


**Figure 7. Threshold gold thickness detail detection curves for plane 23, at AEC dose level for ‘QC’ and ‘clinical’ modes, and half and double AEC dose level for QC mode. Error bars indicate 95% confidence limits**

**Table 5. Threshold gold thickness for reconstructed focal plane 23. The values quoted are the fit to predicted human data. Errors are two standard errors in the mean**

Detail diameter (mm)	Threshold gold thickness (µm)			
	QC mode (1.03 mGy)	Clinical mode (2.06 mGy)	QC mode (2.06 mGy)	QC mode (4.12 mGy)
0.1	2.042±0.247	1.676±0.129	1.574±0.121	0.993±0.120
0.25	0.382±0.043	0.286±0.022	0.281±0.021	0.235±0.027
0.5	0.172±0.024	0.129±0.012	0.129±0.012	0.110±0.015
1.0	0.096±0.022	0.078±0.011	0.078±0.011	0.064±0.015

Additionally, the threshold gold thickness detail detection curves were calculated for planes at 0.5mm intervals and 10mm slabs as shown in Figure 8.



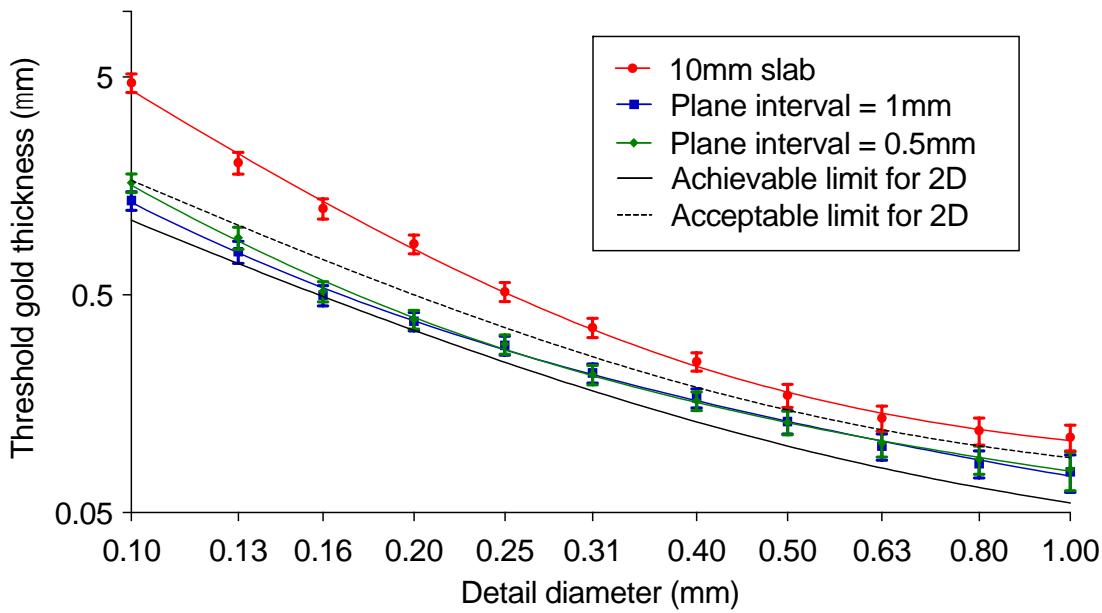


**Figure 8. Threshold gold thickness detail detection curves for 10mm slabs, 1mm plane interval and 0.5mm plane interval at the AEC dose level in QC mode. Error bars indicate 95% confidence limits**

### 3.3 Geometric distortion and resolution between focal planes

#### 3.3.1 Height of best focus

All balls within each image were brought into focus at the same height ( $\pm 1$ mm) above the table.

The number of focal planes reconstructed is equal to the indicated breast thickness plus 4. It was found that 3 additional planes are reconstructed below the breast support, and 1 above the base of the compression paddle.

#### 3.3.2 Positional accuracy within focal plane

No significant distortion or scaling error was seen within focal planes. Scaling errors in both the x and y directions, were found to be less than 0.2%. Maximum deviation from the average distance between the balls was 0.2mm in the x and y direction, compared to the manufacturing tolerance of 0.1mm in the positioning of each ball.

### 3.3.3 Appearance of the ball in adjacent focal planes

In the plane of best focus the balls appeared well defined and circular. Dark areas (reduced pixel value) were seen to the lateral sides of the ball, an effect which is common in tomosynthesis images of this test object and thought to be due to the presence of contrast which exceeds the clinical range. When viewing successive planes, moving away from the plane of best focus, the images of the balls persisted brightly through several focal planes, whilst stretching in the direction parallel to the chest wall edge of the image, forming a faint line which gradually resolved into a row of thirteen spots interspersed with dark patches which persisted through the image. Moving up through the series of focal planes the balls appeared to shift slightly toward the centre of the chest wall edge, as would be expected due to magnification effects. The changing appearance of one of the aluminium balls through successive focal planes is shown in Figure 8.

**Figure 8. Appearance of 1mm aluminium balls in reconstructed focal planes at 3mm intervals from 12mm below to 12mm above the plane of best focus**

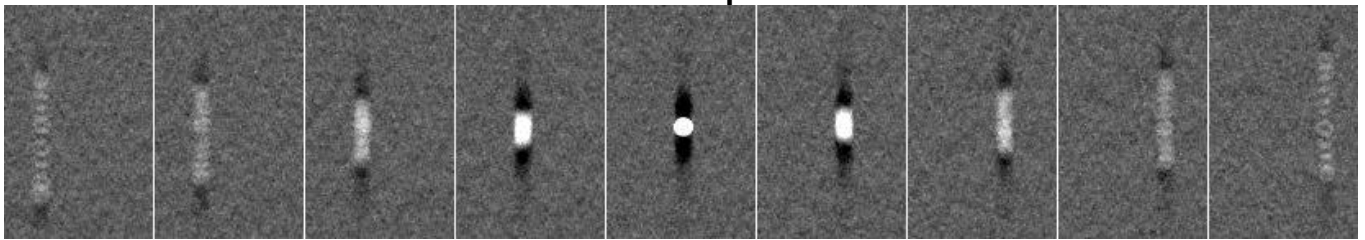
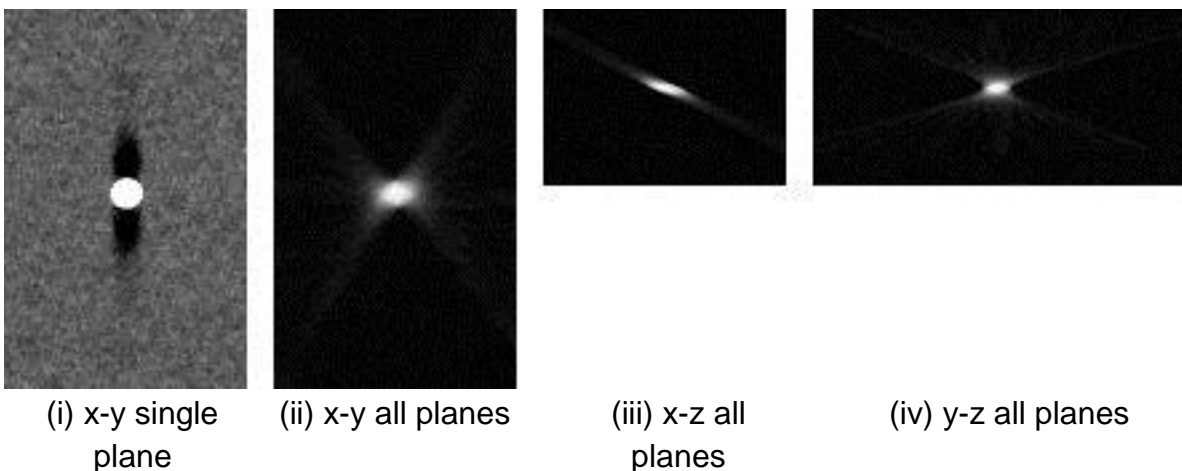


Image extracts for a ball positioned in the central area, 100mm from the chest wall, are shown in Figure 9. In these images, pixels within the focal plane represent dimensions of approximately 0.09mm x 0.09mm, whereas the vertical dimension of each pixel represents the 1mm spacing of the focal planes. Representation of the x-z and y-z planes using square pixels gives an apparent flattening of the balls, whereas in reality reconstruction artefacts associated with these balls extend vertically by a distance exceeding their diameter by more than 10 times.



**Figure 9. Extracts showing 1mm aluminium ball in (i) single focal plane, (ii) the maximum intensity projections through all focal planes, and through re-sliced vertical planes in the directions (iii) parallel and (iv) perpendicular to the chest wall.**

The average z-FWHM of the reconstruction artefact associated with each ball for images of balls at heights of 7.5mm, 27.5mm and 52.5mm above the breast support table was 5.75mm (5.52mm-6.21mm).

### 3.4 Alignment

Alignment at the lateral edges was difficult to measure because the movement of the tube during the scan causes the lateral edges of the X-ray beam to move between projections.

Initially the X-ray beam was found to overlap the front edge of the breast support table, or not extend far enough to cover the whole detector. Later, after a modification to the front collimator, it was found to be satisfactory.

There was no missed tissue at the bottom or top of the reconstructed volume, both with a flat paddle, and with the use of 2mm spacer at the chest wall edge to give some tilt.

### 3.5 Image uniformity and repeatability

Five exposures were made under AEC in tomosynthesis modes at the start of testing and a repeat exposure was made on the second day of testing.

The mAs deviated from the mean value by a maximum of 2.5% for tomosynthesis exposures, within the 5% limiting value in the EUREF protocol.<sup>6</sup>

To test the stability of the reconstruction the SNR was measured just outside the CDMAM grid in the same position in the in-focus plane from 16 reconstructed images of the CDMAM phantom. The SNR deviated from the mean by no more than 2.3%.

The reconstructed images of 45mm PMMA was uniform with no visible artefacts.

### 3.6 Detector response

The detector response for the central projection of the tomosynthesis images acquired at 34kV W/Ag is shown in Figure 10. The incident air kerma at the detector is per projection and therefore one eleventh of the total exposure for the tomosynthesis scan.

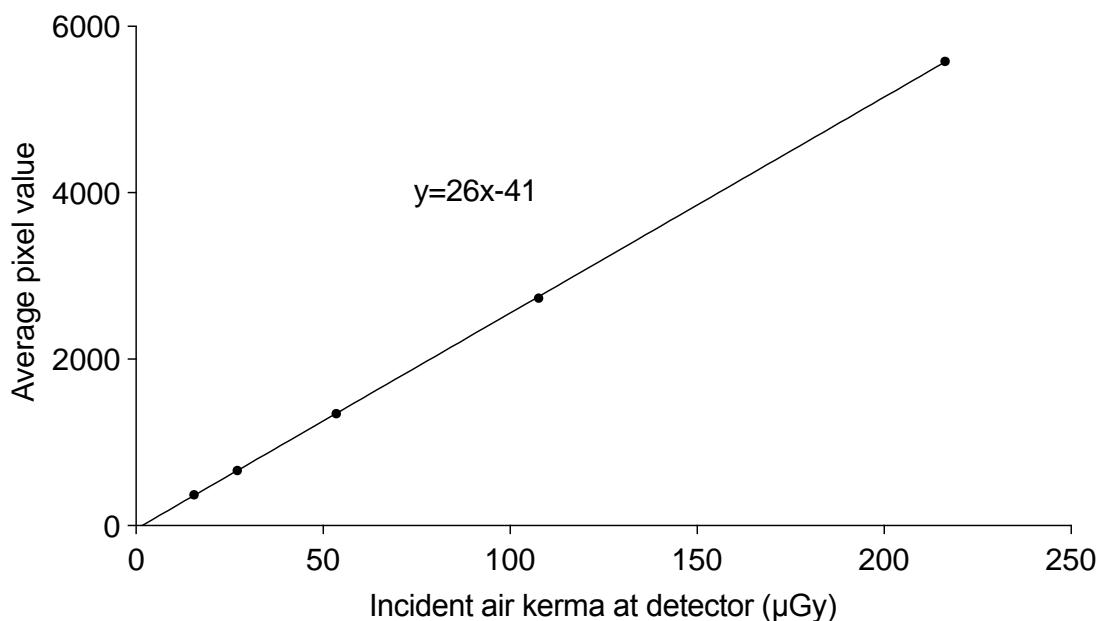


**Figure 10. Detector response in tomosynthesis mode for 34kV W/Ag anode/filter combination with 2mm Al at the tube port**

### 3.7 Timings

Scan times and the times from decompression until the reconstructed tomosynthesis view became available are shown in Table 6 whilst imaging a 53mm equivalent breast, simulated using 45mm PMMA.

**Table 6. Scan and reconstruction timings**

Time from start of exposure until decompression	20s
Time from start of exposure until ready for next exposure	33s
Time from decompression until reconstructed image displayed	1min 55s

### 3.9 Local dense area

Exposures were found to vary with the addition of the small pieces of PMMA, indicating that the AEC does adjust for local dense areas in tomosynthesis mode. The system kept the same target, filter and kV and increased the mAs.

It is generally expected that when the AEC adjusts for locally dense areas, the SNR will remain constant with increasing thickness of extra PMMA. The results obtained with the AEC are presented in Table 7 and Figure 11.

The SNR of each projection images was within 20% of the average SNR as required in EUREF protocol.<sup>6</sup>

**Table 7. AEC performance for local dense area, 0mm from midline and 50mm from the chest wall edge**

Attenuation (mm PMMA)	Target/filter	Tube voltage (kV)	Tube load (mAs)	SNR	% diff from average SNR
0	W/Ag	28	74.7	33.0	0
2	W/Ag	28	75.1	32.4	-2
4	W/Ag	28	83.6	32.6	-2
6	W/Ag	28	88.3	32.8	-1
8	W/Ag	28	95.1	33.4	1
10	W/Ag	28	101.6	33.3	1
12	W/Ag	28	109.1	34.2	3
14	W/Ag	28	112.4	33.2	0

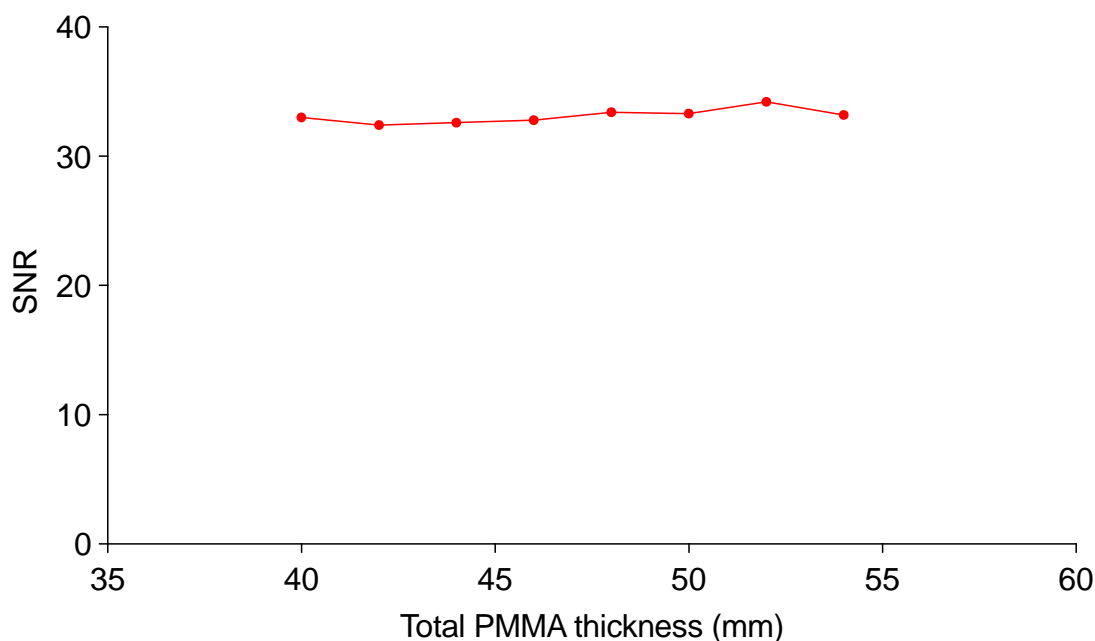


**Figure 11. SNR for local dense area with additional PMMA at 50mm from chest edge**

### 3.9 Radiation safety

The AEC back-up timer for tomosynthesis exposures was originally not functional. This has since been corrected, and retested and found to be functional.

## 4. Discussion

### 4.1 Dose and contrast-to-noise ratio

Tomosynthesis doses were within the limiting values for MGD for tomosynthesis systems in the EUREF protocol.<sup>6</sup> CNR measurements in tomosynthesis projection images showed a decreasing CNR with increasing breast thickness. For tomosynthesis planes the CNR showed little variation with breast thickness.

### 4.2 Image quality

There was no significant difference in threshold gold thickness between 'clinical' and 'QC' modes at normal AEC dose level. At normal dose level the curve of threshold gold thickness with diameter is between the minimum acceptable and achievable levels. At half dose level the threshold gold thickness with diameter is worse than the minimum acceptable level. At double dose, the threshold gold thickness is at the achievable level.

These results take no account of the ability of tomosynthesis to remove the obscuring effects of overlying tissue in a clinical image, and the degree of this effect is expected to vary between tomosynthesis systems.

There is as yet no standard test object that would allow a realistic and quantitative comparison of tomosynthesis image quality between systems or between 2D and tomosynthesis modes is not yet available. A suitable test object would need to incorporate simulated breast tissue to show the benefit of removing overlying breast structure in tomosynthesis imaging, as compared to 2D imaging.

### 4.3 Geometric distortion and reconstruction artefacts

Assessment of geometric distortion images demonstrated that the reconstructed tomosynthesis focal planes were flat and parallel to the surface of the breast support table. No vertical or in-plane distortion was seen and there were no significant scaling errors.

The mean inter-plane resolution (z-FWHM) for the 1mm diameter balls was 5.75mm.

### 4.4 Alignment

Initially the large penumbra of the X-ray field made it impossible to find a suitable position for the front collimator. After a modification, the edge of the field was sharp and alignment was satisfactory.

#### 4.5 Image uniformity and repeatability

The repeatability of tomosynthesis AEC exposures and tomosynthesis reconstructions were found to be satisfactory. The tomosynthesis reconstructions were uniform.

In the combination exposure mode under AEC, the 2D exposure settings selected differed from those selected when using the AEC in 2D mode. This corresponded to around 8% difference in MGD for an equivalent breast thickness of 53mm.

#### 4.6 Reconstruction time

The time from decompression until the reconstructed image displayed was relatively long at 1min 55secs. The reconstruction time was measured using a 45mm thick rectangular phantom of 18x24cm PMMA with 8mm spacers. The reconstruction time for real breasts may be different due to differences in the area and shape.

## 5. Conclusions

The technical performance of the IMS Giotto Class digital breast tomosynthesis system was tested. Performance was found to be satisfactory, though image quality standards have not yet been established for digital breast tomosynthesis systems.

The MGD to the standard breast, in tomosynthesis mode, was found to be 1.58mGy, within the limiting values for digital breast tomosynthesis.

The back-up timer was functional after correction.

Beam alignment at the chest wall edge was satisfactory after a modification was made to the collimator.



## References

1. Strudley CJ, Looney P, Young KC. Technical evaluation of Hologic Selenia Dimensions digital breast tomosynthesis system (NHSBSP Equipment Report 1307 Version 2). Sheffield: NHS Cancer Screening Programmes, 2014
2. Strudley CJ, Warren LM, Young KC. Technical evaluation of Siemens Mammomat Inspiration digital breast tomosynthesis system (NHSBSP Equipment Report 1306 Version 2). Sheffield: NHS Cancer Screening Programmes, 2015
3. Strudley CJ, Hadjipanteli A, Oduko JM, Young KC. Technical evaluation of Fujifilm AMULET Innovality digital breast tomosynthesis system (NHSBSP Equipment Report). Sheffield: NHS Cancer Screening Programmes, 2018
4. Strudley CJ, Oduko JM, Young KC. Technical evaluation of GE Healthcare SenoClaire digital breast tomosynthesis system (NHSBSP Equipment Report 1404). London: Public Health England, 2016
5. Burch A, Loader R, Rowberry B et al. Routine quality control tests for breast tomosynthesis (physicists) (NHSBSP Equipment Report 1407). London: Public Health England, 2015
6. van Engen RE, Bosmans H, Bouwman RW et al. Protocol for the Quality Control of the Physical and Technical Aspects of Digital Breast Tomosynthesis Systems. Version 1.03 [www.euref.org](http://www.euref.org)
7. Dance DR, Young KC, van Engen RE. Estimation of mean glandular dose for breast tomosynthesis: factors for use with the UK, European and IAEA breast dosimetry protocols. *Physics in Medicine and Biology*, 2011, 56: 453-471